Supplementary Information (SI) for Nanoscale.

Supporting Information

Facile synthesis of defective ZnS-ZnO composite nanosheets for efficient piezocatalytic H_2 production

Xiaoxiao Lu,[a] Xiaojing Zhao,[a] Xiangyu Chen,[a] Miaoqiong Xu,[a] Miaoling Huang,[a] Wen-Jie Chen,[a] Yubin Liu,[a*] and Xiaoyang Pan[a*]

[a] College of Chemical Engineering and Materials, Quanzhou Normal University, Quanzhou, 362000, China.

Experimental Section.

DFT calculation:

Density functional theory (DFT) calculations were performed using DMol3 and GGA-PW91. Convergence tolerance (quality: coarse; energy: 1.0 × 10^{-4} Ha; maximum force 0.02 Ha/Å; maximum displacement: 0.05 Å; maximum step size: 0.3 Å). A vacuum gap was set to approximately 50 Å. The calculated perfect (0 0 2) slab model and (4 × 4) supercells consisting of four-fold unit monolayers in the hexagonal P63mc space group. The characteristics of H_2O adsorbed on (0 0 2) surfaces and the presence of S vacancy on (0 0 2) surfaces were investigated. The adsorption energy was calculated with: $E_{ad} = E_{H_2O/slab} - E_{slab} - E_{H_2O}$. E_{slab+H_2O} is the total energy of H_2O adsorbed on (0 0 2) surface, E_{slab} denotes the tatal energy of surface. E_{H_2O} is the energy of an isolated H_2O. According the present definition, a higher value of E_{ad} means stronger energy of absorption.

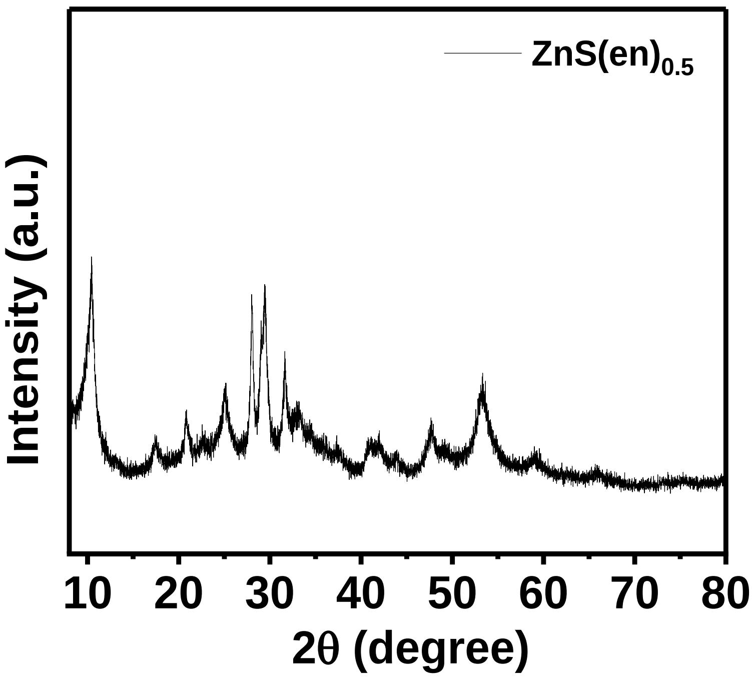

Fig. S1 The XRD patterns of the $ZnS(en)_{0.5}$.

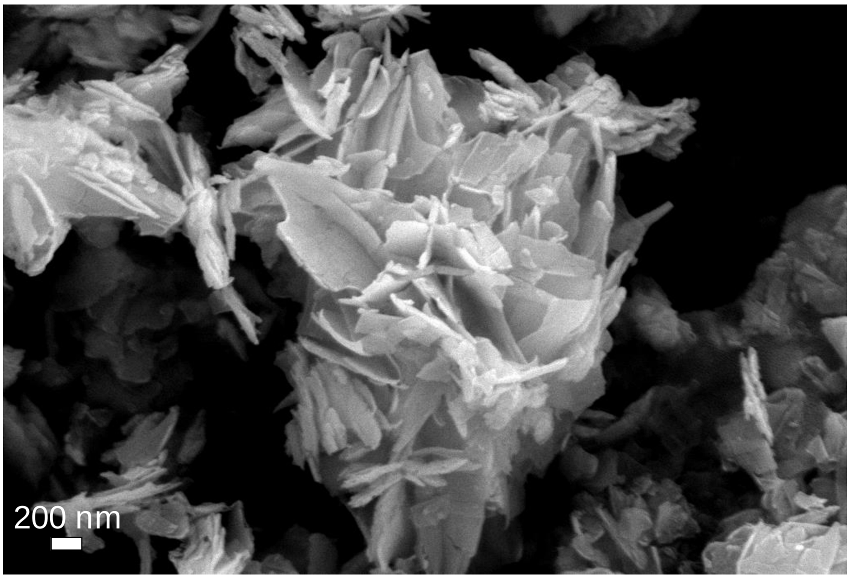

Fig. S2 SEM image of the $ZnS(en)_{0.5}$.

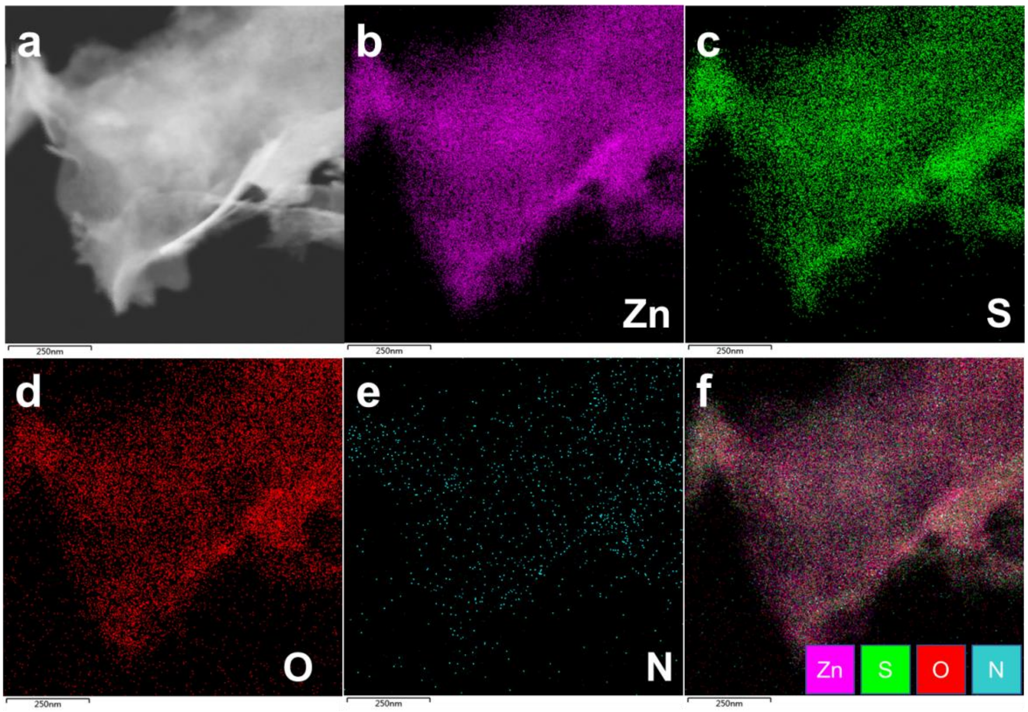

Fig. S3 (a) HAADF-STEM image of ZnS-ZnO; (b-f) Elmental mapping images of ZnS-ZnO.

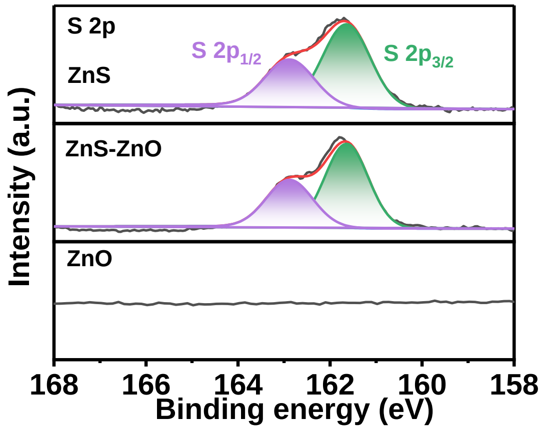

Fig. S4 XPS spectra (S 2p) of the ZnS, ZnS-ZnO and ZnO.

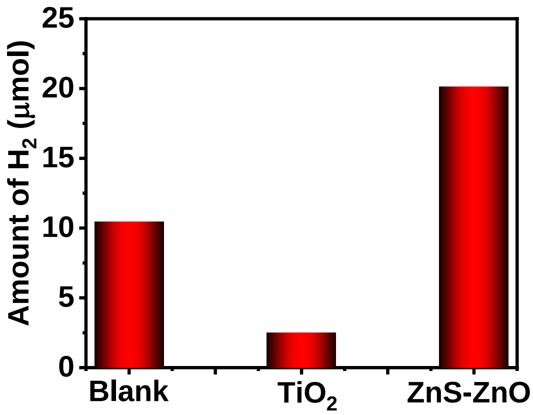

Fig. S5. (b) Average H_2 production in one hour over the samples (300 W, 45kHz, 10vol% CH_3OH).

Note: The blank sample is performed without catalyst. TiO_2 is prepared according to our previous report.[1]

Table S1. Catalytic application for H_2 production driven by Ultrasonic vibration and corresponding experimental parameters.

NO.	Sample	Sample Dosage	Energy Source	H_2 evolution rates (mmol g^{-1} h^{-1})	Refererence
1	ZnS-ZnO	5mg cat 10vol% MeOH	45 kHz，300 W	4.65	This work
2	Zn–N–C dipoles	20 mg cat 7vol% MeOH	2500 r min^{-1}	0.0146	2
3	$(Bi_{0.5}Na_{0.5})TiO_3$	30mg cat 10vol% MeOH	40 kHz	2	3
4	Ti_3C_2/SAMs-NH_2	10 mg cat 0.05 M Na_2SO_3	45 kHz，600 W	0.184	4
5	MoS_2	20 mg cat 0.01M $FeSO_4$	40 kHz，110 W	0.029	5
6	WSe_2	20 mg cat 0.01M $FeSO_4$	40 kHz，110 W	0.011	5
7	$0.7BiFeO_3$–$0.3BaTiO_3$	30mg cat MeOH	40 kHz，100 W	1.322	6
8	$ZnSnO_3$ nanowire	10mg cat 50vol% ethanol	40 kHz,250 W	3.45	7
9	OH-$SrTiO_3$	50 mg cat 20vol% MeOH	40 kHz, 300 W	0.43	8
10	$BiFeO_3$	10 mg cat 0.05M Na_2SO_3	40 kHz，100 W	0.114	9
11	$BaTiO_3$ nanosheet	10mg cat 15vol% triethanolamine	40 kHz，100 W	0.092	10

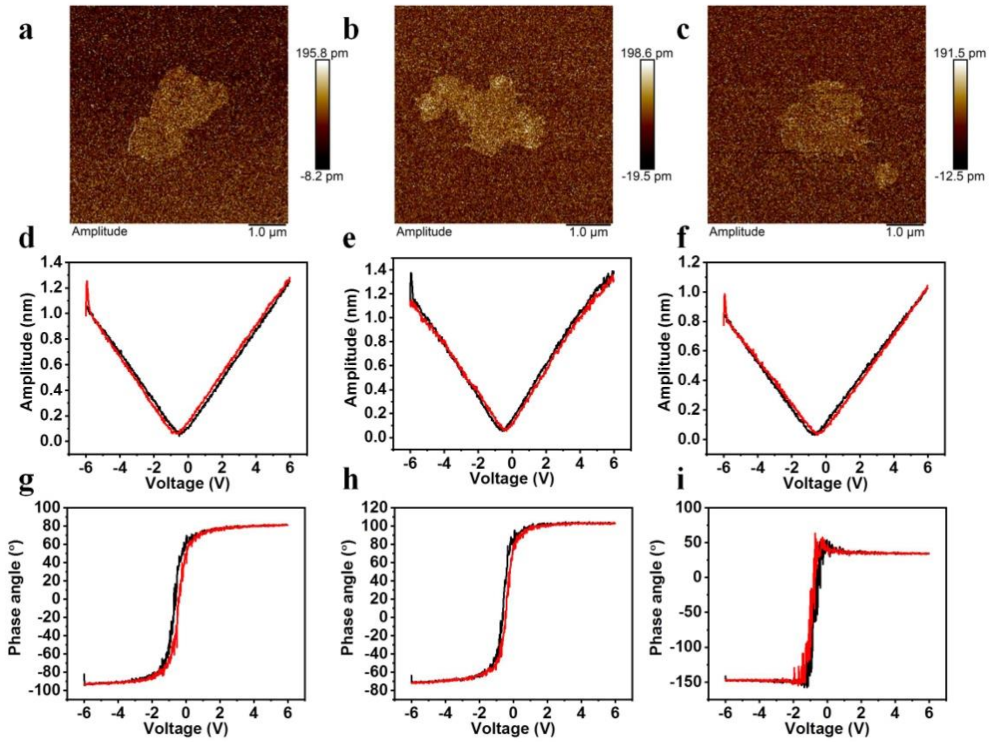

Fig. S6. PFM amplitude image, amplitude loop and the phase switching loop of (a, d, g) ZnS, (b, e, h) ZnS-ZnO and (c, f, i) ZnO.

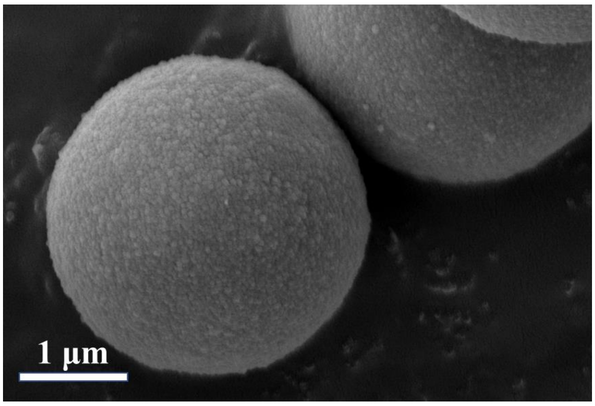

Fig. S7. SEM image of ZnS spheres (ZnS-S).

Note: The sample is synthesized as follows. 768 mg of $Zn(Ac)_2 \cdot 2H_2O$, and 404 mg of NH_2CSNH_2 were dissolved in 70 mL of H_2O and 10 mL of $C_2H_8N_2$. After stirring vigorously for 30 min, the solution was transferred to a 100 mL Teflon-lined stainless steel autoclave and kept at 160 ℃ for 10 h. After cooling to room temperature, the precipitate was collected by centrifugation and washed with ultrapure water and anhydrous ethanol (3 times). Finally, it was dried in a vacuum oven at 60 ℃ overnight.

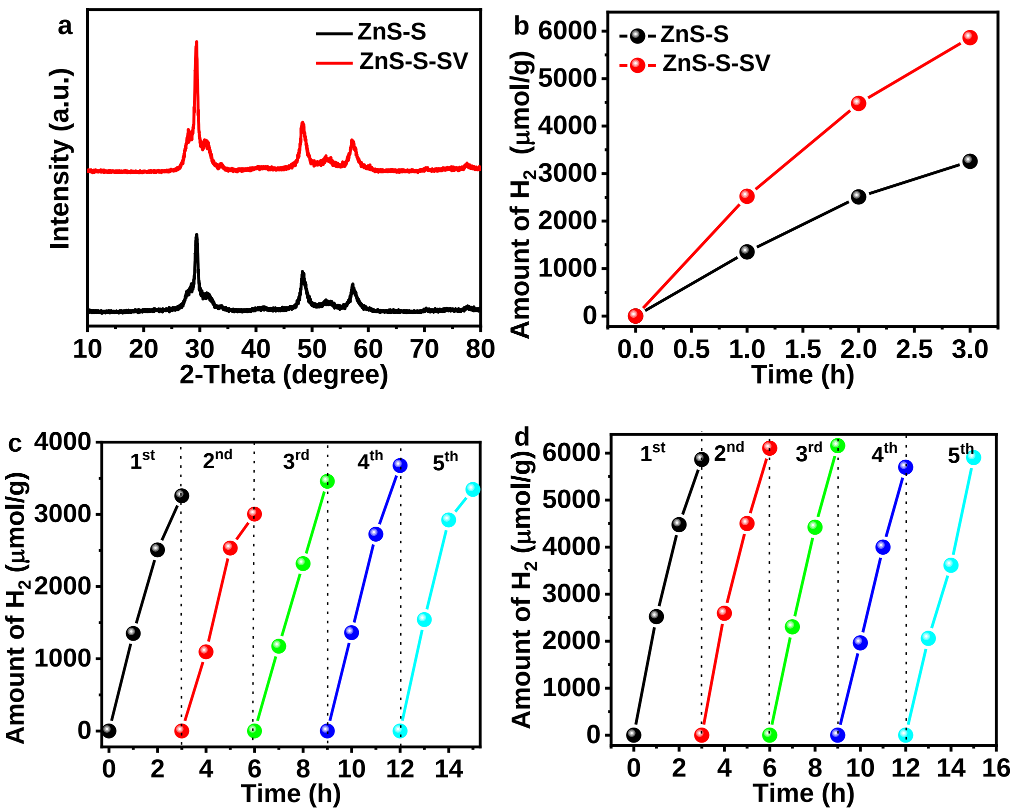

Fig. S8. (a) XRD patterns of ZnS spheres (ZnS-S) and ZnS spheres with sulfur vacancy (ZnS-S-SV); (b) piezocatalytic H_2 production over the samples (300 W, 45k Hz); (c) Stability test of the piezocatalytic H_2 production of ZnS-S at 45 kHz and 300 W; (d) Stability test of the piezocatalytic H_2 production of ZnS-S-SV at 45 kHz and 300 W.

Note: ZnS spheres with sulfur vacancy (ZnS-S-SV) was synthesized by thermal treatment of ZnS-S at 400 ℃ for 2 hours under N_2 atmospheres.

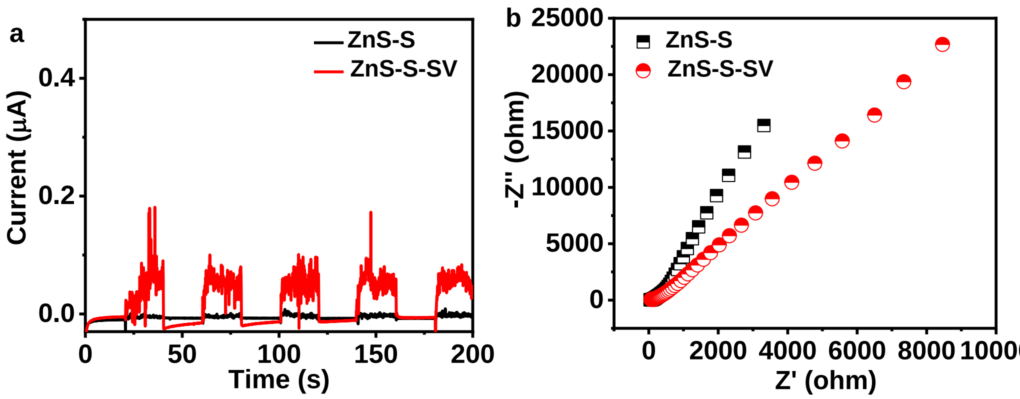

Fig. S9. (a) Piezo-current response of ZnS spheres (ZnS-S) and ZnS spheres with sulfur vacancy (ZnS-S-SV); (b) EIS Nyquist plots of the samples.

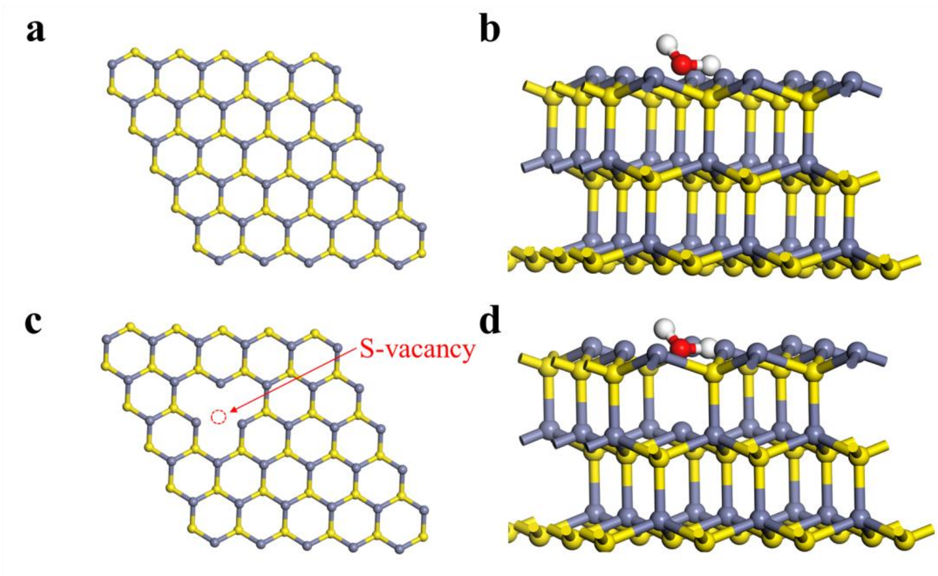

Fig. S10. (a) (002) surface of ZnS; (b) H_2O adsorption on (002) surface of ZnS; (c) (002) surface of ZnS with S vacancy; (d) H_2O adsorption on (002) surface of ZnS with S vacancy.

Table S2. Adsorption energy of H_2O on (002) surface of ZnS.

	Total Energy before adsorption /Ha	**Total energy after adsorption /Ha**	**Adsorption energy /eV**
ZnS	-58803.46	-58879.96	-2.14
ZnS with S vacancy	-58405.18	-58481.66	-3.05

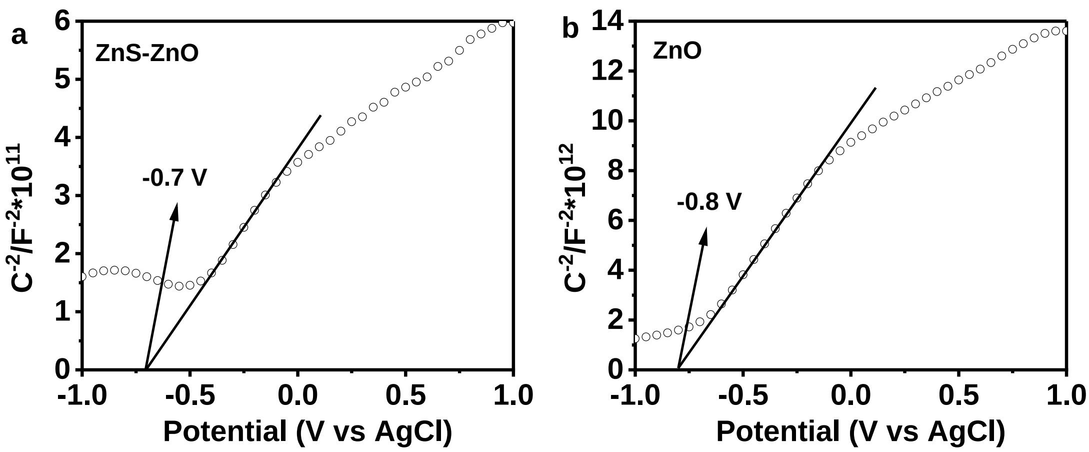

Fig. S11 Mott-Schottky plot of the ZnS-ZnO (a), ZnO (b).

References

1. Pan, X.; Gao, X.; Chen, X.; Lee, H. N.; Liu, Y.; Withers, R. L.; Yi, Z., *ACS Catal.* **2017,** *7* (10), 6991-6998.

2. Hu, P.; Xu, Y.; Lei, Y.; Yuan, J.; Lei, R.; Hu, R.; Chen, J.; Xu, D.; Zhang, S.; Liu, P.; Zhang, X.; Qiu, X.; Feng, W., *J. Energy Chem.* **2022,** *69*, 115-122.
3. Liu, D.; Sun, X.; Tan, L.; Zhang, J.; Jin, C.-C.; Wang, F., *Ceram. Inter.* **2023,** *49* (12), 20343-20350.
4. Wang, S.; Tian, W.; Han, J.; Li, N.; Chen, D.; Xu, Q.; Li, H.; Lu, J., *ACS Appl. Mater. Interfaces* **2023,** *15* (47), 55129-55138.
5. Sun, Y.; Li, X.; Vijayakumar, A.; Liu, H.; Wang, C.; Zhang, S.; Fu, Z.; Lu, Y.; Cheng, Z.; *ACS Appl. Mater. Interfaces*, **2021,** *13*, 11050-11057.
6. Sun, Y.; Li, X.; Vijayakumar, A.; Liu, H.; Wang, C.; Zhang, S.; Fu, Z.; Lu, Y.; Cheng, Z., *ACS Appl. Mater. Interfaces* **2021,** *13* (9), 11050-11057.
7. Wang, Y.-C.; Wu, J. M., *Adv. Fun. Mater.* **2020,** *30* (5), 1907619.
8. Jiang, Y.; Xie, J.; Lu, Z.; Hu, J.; Hao, A.; Cao, Y., *J. Colloid and Interface Sci.* **2022,** *612*, 111-120.
9. Yang, G.; Chen, Q.; Wang, W.; Wu, S.; Gao, B.; Xu, Y.; Chen, Z.; Zhong, S.; Chen, J.; Bai, S., *ACS Appl. Mater. Interfaces* **2021,** *13* (13), 15305-15314.
10. Yu, C.; Tan, M.; Li, Y.; Liu, C.; Yin, R.; Meng, H.; Su, Y.; Qiao, L.; Bai, Y., *J. Colloid and Interface Sci.* **2021,** *596*, 288-296.